

Characteristics of GaN grown on 6H-SiC with different AlN buffers*

Ding Guojian(丁国建)[†], Guo Liwei(郭丽伟), Xing Zhigang(邢志刚), Chen Yao(陈耀),
Xu Peiqiang(徐培强), Jia Haiqiang(贾海强), Zhou Junming(周均铭),
and Chen Hong(陈弘)

(Beijing National Laboratory of Condensed Matter Physics, Institute of Physics, Chinese Academy of Sciences, Beijing 100190, China)

Abstract: Characteristics of GaN grown on 6H-SiC (0001) substrates using different thicknesses of AlN buffers are studied. It is found that the surface morphology and crystal quality of GaN film closely depends on the strain state of the AlN buffer. For a thicker AlN buffer, there are cracks on GaN surface, which make the GaN films unsuitable for applications. While for a thinner AlN buffer, more dislocations are produced in the GaN film, which deteriorates the performance of GaN. Possible generation mechanisms of cracks and more dislocations are investigated and a ~ 100 nm AlN buffer is suggested to be a better choice for high quality GaN on SiC.

Key words: GaN; AlN; XRD; MOCVD

DOI: 10.1088/1674-4926/31/3/033003

PACC: 7280E; 6855

1. Introduction

AlGaIn/GaN high-electron mobility transistors (HEMTs) are very promising for high temperature, high frequency and high power microwave device applications owing to their superior material properties^[1]. A high quality GaN film is essential for device fabrication. Due to the lack of sufficiently high quality bulk GaN substrate, the growth of GaN epitaxial layer has so far been carried out on various foreign substrates such as sapphire and silicon carbide (SiC). Most commercially available GaN-based devices are normally grown on sapphire substrates because of the relatively low cost and general availability, although their lattice parameter and coefficient of thermal expansion are significantly different from that of GaN. For power device applications, however, it is desirable for a substrate with higher thermal conductivity, such as SiC. 6H-SiC has a thermal conductivity coefficient (room temperature) of 4.9 W/(cm·K), which is an order of magnitude higher than sapphire (0.5 W/(cm·K))^[2]. Meanwhile, SiC also has a lower lattice mismatch to GaN ($\sim 3.5\%$) and AlN ($\sim 1\%$) compared to sapphire^[3]. However, the thermal expansion coefficient of 6H-SiC (4.2×10^{-6} K⁻¹) is lower than that of GaN (5.59×10^{-6} K⁻¹), which produces a strain of $\sim 0.1\%$ for a growth temperature of 1000 °C^[4]. As a result, GaN layers grown directly on SiC (0001) are usually under tensile strain at room temperature and there are high amounts of dislocations and even cracks in the GaN films caused by strain. To resolve the problems, an AlN buffer layer has been widely used to reduce this tensile strain and even producing compressively strained GaN layers grown on SiC^[5-8] and AlN buffer has been repeatedly found to be necessary to achieve a GaN layer with a smooth surface and a reasonably low density of threading dislocations via the metal organic chemical vapor deposition technique (MOCVD)^[2, 9].

Although remarkable progress on the research of Al-

GaN/GaN HEMT structures grown on SiC substrate has been made, few studies are focused on the influence of AlN buffer layers on GaN features, especially on the residual stress in GaN film and the accompanying effects that produced serious characteristics in the GaN layer. In this paper, we study the growth of GaN films by MOCVD on (0001) 6H-SiC substrates with different AlN buffers in thickness and focus on the residual strain in the thick GaN epilayers and the effects on its morphology and crystal quality.

2. Experiment

Substrates used in this study are on-axis 6H-SiC (0001). The GaN/AlGaIn heterostructures were grown on 6H-SiC substrates sandwiched with different thickness of AlN buffer layers. Trimethylgallium (TMGa), trimethylaluminum (TMAI) and ammonia (NH₃) were used as Ga, Al and N precursors, respectively. Before the growth initiation, the substrates were subjected to an in situ H₂ atmosphere at 1100 °C for 10 min. Then, the AlN buffer layers of different thickness were deposited respectively, on which the GaN/AlGaIn heterostructure structures were grown in sequence of a ~ 2 - μ m-thick GaN buffer layer and a ~ 25 -nm-thick AlGaIn (28% Al) barrier layer. During the growth of AlN and AlGaIn, reactor pressure was maintained at 70 mbar to reduce parasitic reaction and increase the incorporation efficiency of Al into AlGaIn films. All layers were grown with unintentional doping. Here, three samples of A, B and C were prepared with AlN buffer in thicknesses of 250, 100, and 32 nm respectively. Except the thickness of AlN buffers, all of the other growth conditions were kept the same for the three samples.

After growth, high-resolution X-ray diffraction (HRXRD) was performed to characterize the structural quality and strain state of the samples by the Bede D1 system. Cross-sectional

* Project supported by the National Natural Science Foundation of China (No. 10574148), the National High-Tech Research and Development Program of China (Nos. 2006AA03A106, 2006AA03A107), and the State Key Development Program for Basic Research of China (No. 2006CB921300).

[†] Corresponding author. Email: dingguojian@126.com

Received 1 September 2009, revised manuscript received 23 October 2009

© 2010 Chinese Institute of Electronics

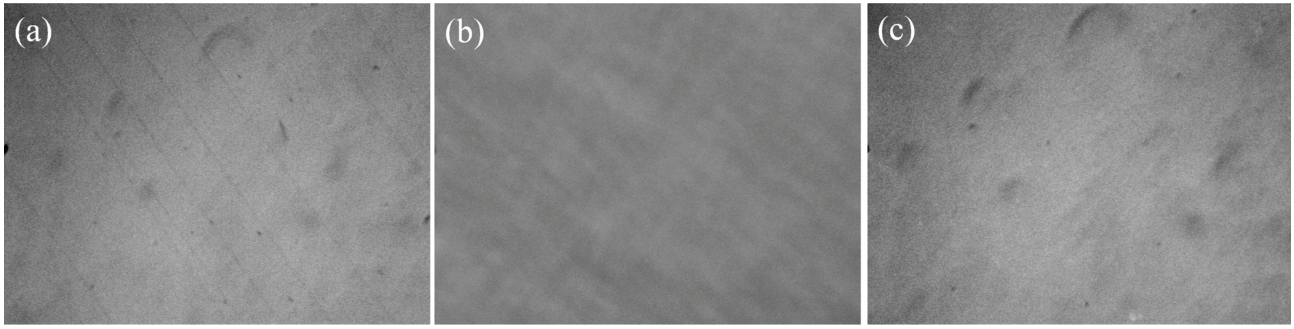


Fig. 1. 200 times magnified optical microscope images of (a) sample A, (b) sample B, and (c) sample C.

Table 1. Detailed characteristics of the three samples: AlN buffer thickness, FWHMs of XRD peaks, surface roughness and E_2 phonon modes of GaN and AlN layers.

Sample	Thickness of AlN buffer (nm)	Crack	FWHM (0002) (arcsec)	FWHM ($10\bar{1}2$) (arcsec)	Roughness $10 \times 10 \mu\text{m}^2$ (nm)	E_2 phonon mode (cm^{-1})	
						AlN	GaN
A	250	yes	370	375	0.73	661.3	567.8
B	100	no	184	275	0.31	662.1	565.8
C	32	no	257	342	0.74	–	567.8

transmission electron microscopy measurement (TEM) was performed with a JEOL 2010 system operated at 200 keV to study dislocations in selected samples. The process of preparing TEM specimens was described elsewhere^[10]. Surface morphology was characterized using contrast enhanced optical microscopy (OLMPUS-BHM) and atomic force microscopy (AFM). Raman scattering measurements were carried out at room temperature to assess the mean strain state of the samples, where the used wavelength of the excited light source is 532 nm produced by a frequency-doubled Nd:YAG laser and scattered light was analyzed by a triple JY-HR800 (France) spectrometer connected to computer-controlled systems for scanning and data acquisition.

3. Results and discussion

In our early experiments, it was found that GaN films grown on SiC with low temperature (~ 650 °C) AlN buffer layers show cracks on the surface. According to Warren Weeks *et al.*^[2] a high temperature (~ 1100 °C) is essential for an AlN buffer layer to promote the growth of monocrystalline AlN for a high quality GaN film. Therefore, the samples discussed here were all grown on high temperature AlN buffer layers to satisfy requirements for high quality GaN growth. The optical microscope images of the samples show a crack-free smooth surface for samples B and C, and cracks for sample A. Figures 1(a), 1(b) and 1(c) show the 200 times magnified surface images of samples A, B and C respectively. It can be seen that there exist cracks on the surface of sample A and the cracks are all along the $\langle 11\bar{2}0 \rangle$ direction with average spaces about ten to twenty micrometers. No regrowth of GaN was seen on the cracks, indicating that the cracks were generated after the epitaxy, probably while cooling.

For GaN layers grown directly on SiC (0001), the strain state of GaN can be thought of as a superposition of compression from the lattice mismatch and tension from the ther-

mal mismatch relative to the SiC substrate. Both the lattice constant and the thermal expansion coefficient of SiC in the basal plane are smaller than those of GaN^[11–13]. GaN layer was compressively strained at a typical growth temperature of ~ 1000 °C because of the lattice mismatch until the layer thickness reached the critical thickness, while a 33.1% mismatch in the thermal expansion coefficient between GaN and SiC produced a trend of tensile strain^[2]. For a thicker GaN layer, the adjustment of compressive strain caused by lattice mismatch happened at growth temperature. Then after growth, tensile strain introduced by the mismatch of the thermal expansion coefficient was generated during cooling process. As a result, cracks are often observed in GaN films whose thickness is over $1 \mu\text{m}$ grown on SiC (0001). The use of an AlN buffer layer may reduce this tensile strain and even compressively strained GaN layers on SiC have been reported^[5–8]. In the case of GaN grown on AlN/SiC, according to Einfeldt *et al.*^[14] part of the compressive strain in GaN remains even when its thickness is over the critical thickness. The stress relief is not abrupt but happens gradually in a wide thickness range. Even if GaN film thickness is over $1 \mu\text{m}$, its residual strain is about one tenth of the 3.4% lattice mismatch in the film remained^[8]. During the postgrowth cooling, the residual compressive strain in the film will compensate the tensile strain resulted from the mismatch in thermal expansion coefficients between GaN and SiC, which will be beneficial to obtaining crack-free GaN films. The reasons for generating cracks in the sample A will be discussed after the analysis on the strain state of the samples based on XRD diffraction.

Crystal quality and strain states of the GaN films in three samples are studied by XRD and Raman scattering experiments. The details of the crystal quality of the three samples represented by full width at half maximum (FWHM) of XRD symmetry (0002) and asymmetry ($10\bar{1}2$) diffraction, and surface roughness measured by AFM under scan area of $10 \times 10 \mu\text{m}^2$ are listed in Table 1. It is noted that samples B and C

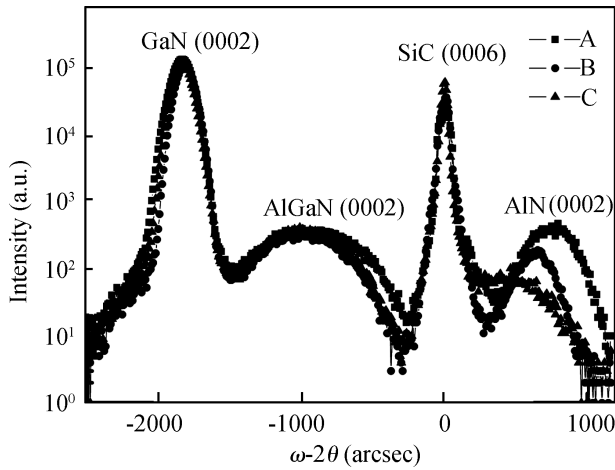


Fig. 2. (0002) diffraction of XRD profiles for the three samples with 250 nm (sample A), 100 nm (sample B) and 32 nm (sample C) AlN buffer layers.

without cracks show relatively small FWHMs for both (0002) and (10 $\bar{1}$ 2) plane diffractions, and sample B has the narrowest FWHMs and the flattest surface. As is well known, FWHM of XRD symmetric and asymmetric diffraction indirectly reflects threading dislocation (TD) density of a different type. The FWHM of symmetric (0002) is sensitive to the density of pure screw and mixed TD, while the FWHM of asymmetric (10 $\bar{1}$ 2) is sensitive to the pure edge and mixed TD^[15]. The results suggest that the sample B possesses the best crystal quality, and also hints that the 100 nm AlN buffer layer is a better choice for GaN growth on SiC, that has been widely adopted in fabricating GaN based microwave device materials^[3].

Strain states of these three GaN films were measured using (0002) plane XRD profiles as shown in Fig. 2. For completely relaxed GaN and AlN on SiC, separation of the diffraction peaks between SiC (0006) and GaN (0002) is $\Delta(\theta_0)_{\text{SiC-GaN}} = 1849.32$ arcsec, and that between SiC (0006) and AlN (0002) is $\Delta(\theta_0)_{\text{AlN-SiC}} = 771.3$ arcsec. For samples A and C, the separations of $\Delta(\theta)_{\text{SiC-GaN}}$ are 1835 and 1836 arcsec, respectively, which means very little tensile strain existed in these two GaN layers, or in other words, the GaN layers are nearly completely relaxed. While a separation of $\Delta(\theta)_{\text{GaN-SiC}} = 1817$ arcsec for sample B means a relatively large tensile strain of the GaN layer. Furthermore, the separations of $\Delta(\theta)_{\text{AlN-SiC}}$ are 733, 643 and 535 arcsec for samples A, B and C, respectively, that correspond to their relaxation degrees relative to SiC substrates that are 92.3%, 68.5% and 34.2% respectively. This means that all the AlN layers in these three samples suffer from more or less compressive strain on basal plane. Among these three samples, AlN in sample A is nearly completely relaxed and provides a relative small compressive stress on GaN grown on it compared with that in the other two samples. In the case, the resultant tensile strain in the GaN layer during cooling after growth is so large that cracks are generated in the film, which is clearly observed on its surface as shown in Fig. 1(a).

A quantitative discussion on stress is given for sample B. Taking the SiC substrate (0006) diffraction peak as a standard, the out-of-plane lattice constants C_{ex} of GaN and AlN of sample B can be deduced from the separations of the peaks rela-

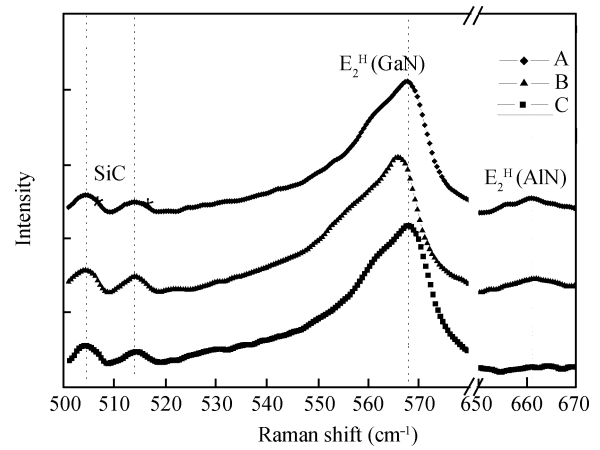


Fig. 3. Raman spectra near the E₂ phonon modes from GaN and AlN layers of samples A, B and C. The asterisks mark the Raman peaks of SiC substrate.

tive to SiC (0006) peak. The deduced $C_{\text{GaN-ex}}$ and $C_{\text{AlN-ex}}$ are about 0.5181 nm and 0.4990 nm, respectively. So the strain in GaN and AlN layer can be deduced from the relations $\epsilon_c = (C_{\text{ex}} - C_0)/C_0$, and $\epsilon_c/\epsilon_a = -2C_{13}/C_{33}$, where ϵ_a and ϵ_c are strains on basal plane and along growth direction, C_0 is the fully relaxed lattice constant and stress is deduced from the equation:^[16]

$$\sigma_a = \left(C_{13} - \frac{C_{11}C_{33}}{2C_{13}} - \frac{C_{12}C_{33}}{2C_{13}} \right) \epsilon_c. \quad (1)$$

By using the bulk lattice constants of GaN ($C_{0\text{GaN}} = 0.5185$ nm) and AlN ($C_{0\text{AlN}} = 0.4982$ nm), and the elastic constants C_{ij} of GaN ($C_{11} = 390$ GPa, $C_{12} = 145$ GPa, $C_{13} = 106$ GPa, and $C_{33} = 398$ GPa) and AlN ($C_{11} = 345$ GPa, $C_{12} = 125$ GPa, $C_{13} = 120$ GPa, and $C_{33} = 395$ GPa)^[17], biaxial stresses on the basal plane are obtained as 0.62 GPa and -1.04 GPa for GaN and AlN in sample B, respectively.

Furthermore, the strain in GaN and AlN layers is also analyzed based on the shift of E₂ phonon mode in Raman scattering measurements. As is well known, E₂ mode is sensitive to biaxial stress^[18]. Figure 3 displays the Raman spectra of GaN and AlN layers near E₂ mode for samples A, B and C. The asterisks mark Raman peaks of 6H-SiC substrate, which is used as a standard to calibrate errors produced during Raman measurements. It is noted that the E₂ phonon modes for GaN in samples A and C are nearly all located at 567.8 cm⁻¹, which is nearly the same to bulk GaN E₂ mode of 567.6 cm⁻¹^[19]. The results sufficiently support the conclusion that GaN are nearly completely relaxed deduced from Fig. 2. However, E₂ phonon mode of GaN in sample B is located at 565.8 cm⁻¹, a 2 cm⁻¹ shift exists towards low frequency. The result suggests a relatively large strain remained in GaN layer in sample B, consisting with the result deduced from Fig. 2. The E₂ phonon modes of AlN layers are 661.3 cm⁻¹ and 662.1 cm⁻¹ respectively for samples A and B, and it is not easy to determine for sample C due to its E₂ mode is too weak to identify. The shift to high frequency of the E₂ phonon modes for samples A and B compared with bulk AlN phonon mode of 657.4 cm⁻¹ indicates that compressive strain existed in the AlN layers consisted with the results deduced from XRD.

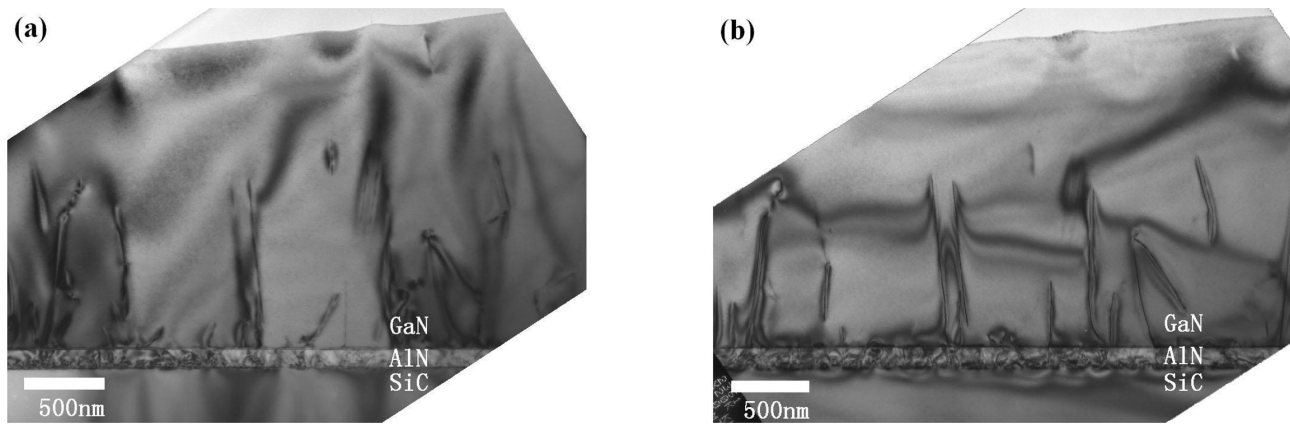


Fig. 4. Two-beam bright field cross-sectional TEM images of sample B with diffraction vectors along (a) $g = 002$ and (b) $g = 110$.

A quantitative discussion on stress based on the Raman shift is given and compared with the results deduced from XRD data given above. According to a relation between stress and strain $\Delta\omega = k\sigma_a^{[20]}$, stress on basal plane is deduced, where $\Delta\omega$ is Raman shift in phonon energy due to biaxial stress. Tensile or compressive stress corresponds to a $\sigma_a > 0$ or $\sigma_a < 0$. Here Raman-stress factor k for E_2 phonon is $-3.4 \pm 0.3 \text{ cm}^{-1}/\text{GPa}$ for GaN^[21] and $-6.3 \pm 1.4 \text{ cm}^{-1}/\text{GPa}$ for AlN^[20], respectively. The stress is calculated as 0.58 GPa for GaN as taking k as $-3.1 \text{ cm}^{-1}/\text{GPa}$ and -0.96 GPa for AlN as k is $-4.9 \text{ cm}^{-1}/\text{GPa}$ in sample B. The stress values deduced here are consistent with the results based on XRD data considering the errors of measurement and calculation.

Analyzing the results presented above, it is noted that the strain relaxation degree of the GaN layer in sample B is less sufficient compared with that in samples A and C. Usually stress is released by cracks or generating dislocations. For sample A, cracks and dislocations release its stress, while forming more dislocations releases stress for samples B and C. However, the stress is not sufficiently released in sample B compared with that in sample C. Therefore, dislocation density in sample B is lower than that in sample C, which is supported by the narrower XRD FWHMs of (0002) and (10 $\bar{1}$ 2) diffractions for sample B compared with sample C as listed in Table 1. According to Moran^[3], AlN is grown on SiC nucleates via the islands coarsening method, and tends to coalesce gradually and reaches completely coalescence after growing to ~ 100 nm thickness. For sample C, a 32-nm-thick AlN layer probably is partially coalesced islands with an accident surface. As GaN growth is beginning on the surface, GaN prefer to nucleate at the undulations and pits of the AlN surface as observed by Nishida *et al.*^[22]. Therefore, higher GaN nucleation islands formed on the AlN surface of sample C than that of sample B, leading to a higher TD density in sample C, as is known that the majority of TDs tend to generate at coalescent boundaries of the islands.

The dislocation in sample B was further studied by TEM. Figure 4 presents two-beam bright field cross-sectional TEM images of sample B with diffraction vectors of $g = 002$ and $g = 110$. A sharp and smooth GaN/AlN interface is observed because of GaN and AlN having a similar crystal structure and electronic configuration, as opposed to AlN and SiC. Meanwhile, it is noted that there exists a high density of TDs in

the AlN buffer layer. However, both the screw dislocations and the edge dislocations decrease sharply in the GaN layer. A lower TD density in the GaN layer means a high crystal quality, which is consistent with the narrower XRD FWHM values of GaN in sample B. A high crystalline quality and smooth hetero-junction interface will be beneficial to a better performance of the GaN/AlGaIn heterostructure. Hall measurements on sample B at room temperature showed a mobility of $1800 \text{ cm}^2/(\text{V}\cdot\text{s})$ with a sheet carrier density of $1.3 \times 10^{13} \text{ cm}^{-2}$, which further confirms that the ~ 100 -nm-thick AlN buffer is a better choice for GaN grown on SiC.

4. Conclusion

In conclusion, characteristics of GaN grown on 6H-SiC (0001) substrates using different thicknesses of AlN buffer are studied. The close relationships of AlN buffer layer thickness, strain states of GaN and AlN, and stress release ways and related surface morphology are revealed. For a thicker AlN buffer, there are cracks on the GaN surface that make the GaN films unsuitable for application. While, for a thinner AlN buffer, more dislocations produced in the GaN films deteriorates the performance of the GaN. It is found that a ~ 100 -nm-thick AlN buffer, whose strains are relaxed near 70%, is an optimizing choice for GaN grown on 6H-SiC substrate for application in microwave devices.

References

- [1] Ambacher O, Smart J, Shealy J R, et al. Two-dimensional electron gases induced by spontaneous and piezoelectric polarization charges in N- and Ga-face AlGaIn/GaN heterostructures. *J Appl Phys*, 1999, 85: 3222
- [2] Weeks T W, Bremser M D Jr, Ailey K S, et al. GaN thin films deposited via organometallic vapor phase epitaxy on α -(6H)-SiC(0001) using high-temperature monocryalline AlN buffer layers. *Appl Phys Lett*, 1995, 67: 401
- [3] Moran B, Wu F, Romanov A E, et al. Structural and morphological evolution of GaN grown by metalorganic chemical vapor deposition on SiC substrates using an AlN initial layer. *J Cryst Growth*, 2004, 273: 38
- [4] Einfeldt S, Roskowski A M, Preble E A, et al. Strain and crystallographic tilt in uncoalesced GaN layers grown by maskless pendeoepitaxy. *Appl Phys Lett*, 2002, 80: 953

- [5] Davydov V Y, Averkiev N S, Goncharuk I N, et al. Raman and photoluminescence studies of biaxial strain in GaN epitaxial layers grown on 6H-SiC. *J Appl Phys*, 1997, 82: 5097
- [6] Skromme B J, Zhao H, Wang D, et al. Strain determination in heteroepitaxial GaN. *Appl Phys Lett*, 1997, 71: 829
- [7] Perry W G, Zheleva T, Bremser M D, et al. Correlation of biaxial strains, bound exciton energies, and defect microstructures in GaN films grown on AlN/6H-SiC(0001) substrates. *J Electron Mater*, 1997, 26: 224
- [8] Waltereit P, Brandt O, Trampert A, et al. Influence of AlN nucleation layers on growth mode and strain relief of GaN grown on 6H-SiC(0001). *Appl Phys Lett*, 1999, 74: 3660
- [9] Weeks T W, Bremser M D Jr, Ailey K S, et al. Undoped and doped GaN thin films deposited on high-temperature monocrystalline AlN buffer layers on vicinal and on-axis α (6H)-SiC(0001) substrates via organometallic vapor phase epitaxy. *J Mater Res*, 1996, 11: 1011
- [10] Xing Z G, Wang J, Wang Y, et al. Crystallographic wing tilt and thermal-stress distribution of GaN laterally overgrown on maskless V-grooved sapphire substrate by metal-organic chemical vapor deposition. *J Vac Sci Technol B*, 2007, 25: 697
- [11] Bykhovski A D, Gelmont B L, Shur M S. Elastic strain relaxation in GaN-AlN-GaN semiconductor-insulator-semiconductor structures. *J Appl Phys*, 1995, 78: 3691
- [12] Grandjean N, Massies J. GaN and $\text{Al}_x\text{Ga}_{1-x}\text{N}$ molecular beam epitaxy monitored by reflection high-energy electron diffraction. *Appl Phys Lett*, 1997, 71: 1816
- [13] Damilano B, Grandjean N, Semond F, et al. From visible to white light emission by GaN quantum dots on Si (111) substrate. *Appl Phys Lett*, 1999, 75: 962
- [14] Einfeldt S, Reitmeier Z J, Davis R F. Surface morphology and strain of GaN layers grown using 6H-SiC (0001) substrates with different buffer layers. *J Cryst Growth*, 2003, 253: 129
- [15] Heying B, Wu X H, Keller S, et al. Role of threading dislocation structure on the X-ray diffraction peak widths in epitaxial GaN films. *Appl Phys Lett*, 1996, 68: 643
- [16] Moram M A, Vickers M E. X-ray diffraction of III-nitrides. *Rep Prog Phys*, 2009, 72: 036502
- [17] Polian A, Grimsditch M, Grzegory I. Elastic constants of gallium nitride. *J Appl Phys*, 1996, 79: 3343
- [18] Perlin P, Jaubertie-Carlton C, Itie J P, et al. Raman scattering and X-ray-absorption spectroscopy in gallium nitride under high pressure. *Phys Rev B*, 1992, 45: 83
- [19] Harima H. Properties of GaN and related compounds studied by means of Raman scattering. *J Phys: Condens Matter*, 2002, 14: R967
- [20] Kisieloeski C, Krüger J, Ruvimov S, et al. Strain-related phenomena in GaN thin films. *Phys Rev B*, 1996, 54: 17745
- [21] Ahmad I, Holtz M, Faleev N N, et al. Dependence of the stress-temperature coefficient on dislocation density in epitaxial GaN grown on α - Al_2O_3 and 6H-SiC substrates. *J Appl Phys*, 2004, 95: 1692
- [22] Nishida T, Kobayashi N. Nucleation control in MOVPE of group III-nitrides on SiC substrate. *J Cryst Growth*, 2000, 221: 297